

An electron-hadron collider at the high-luminosity LHC

K D J André¹, B Holzer¹, L Forthomme² and K Piotrkowski²

¹CERN, Organisation européenne pour la recherche nucléaire, Meyrin, Switzerland

²AGH University of Kraków, Poland

E-mail: laurent.forthomme@cern.ch

Abstract. We discuss a concept of a lower-energy version of the Large Hadron-electron Collider (LHeC), delivering electron-hadron collisions concurrently to the hadron-hadron collisions at the high-luminosity LHC at CERN. Assuming the use of a 20 GeV electron Energy Recovery Linac (ERL), we describe the optimised beam dynamics, accelerator technologies, and detector constraints required for such a "phase-one" LHeC. Finally, we also discuss the ERL configurations, the possibility of delivering electron-hadron collisions during the planned LHC Run5 and briefly outline the scientific potential of this proposal.

1. Introduction

The Large Hadron-electron Collider (LHeC) [1] will open new frontiers in high-energy physics as it will become a unique laboratory for studies of deep-inelastic scattering (DIS) and Higgs boson, electroweak, top quark and BSM phenomena in a vast range of virtualities Q^2 , from very close to zero up to 10^6 GeV², and for a much extended range of x – the fractional longitudinal momentum of partons. An intense electron beam from a novel energy recovery linac (ERL) will collide with a proton or ion beam from the high-luminosity LHC (HL-LHC), in the re-designed P2 interaction region capable of hosting either electron-hadron or hadron-hadron collisions, concurrently with hadron-hadron collisions in other HL-LHC experiments [2].

In the Conceptual Design Report (CDR) of LHeC, it is assumed that a three-pass ERL delivers a 50 GeV high-current electron beam [1]. In this proposal, we assume the use of a 20 GeV single-pass ERL (see Fig. 1) with yet higher beam current of 60 mA, and with a circumference of a third of the LHC's. This choice of design is motivated by the availability of the technology to operate a single-pass ERL (although presently at lower beam currents) and by the overall simplification, in particular, in the design of the adequate machine-detector interface thanks to much lower levels of synchrotron radiation. One should note that the cost of building such a "phase-one" LHeC as well as its running costs are significantly lower than for the final LHeC configuration.

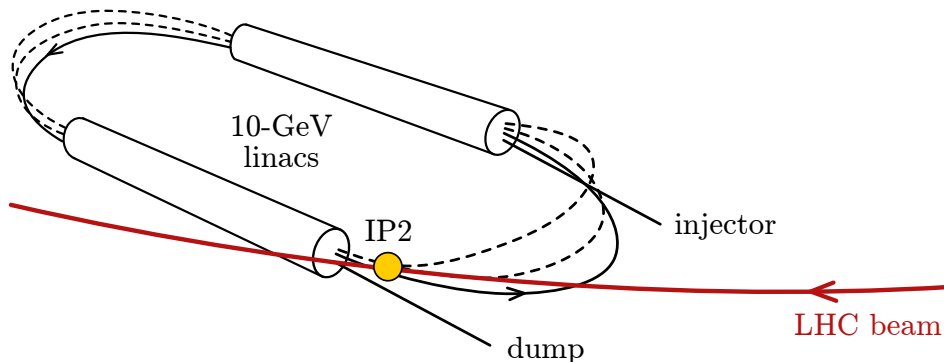


Figure 1. Schematics of the single-pass LHeC layout with the optional return arcs 3 – 6 (dashed lines).

Such a staged realisation of the LHeC project provides a huge benefit not only in reducing financial strains but first of all in the availability of concurrent electron-hadron collisions already during Run5 of the HL-LHC. Consequently, apart from the possibility of performing a wide range of unique and important studies almost 10 years earlier, the results of such a new electron-hadron experiment could also be used to timely improve measurements in other (hadron-hadron) experiments at the HL-LHC.

2. The LHeC interaction region

The fundamental principle of an ERL provides an ideal condition for a staged particle accelerator. Still, a number of items have to be followed up, as beam parameters scale with energy, and so while keeping the general layout untouched, a re-optimisation of the beam dynamics is needed for highest performance of the electron-proton collisions.

Schematically, the concept is shown in Fig. 1 – the geometry of the ERL will remain the same: two superconducting linacs are connected by return arcs on both sides. Details about the general layout can be found in [3] and [4]. However, for the phase-one case with reduced electron energy modules needed to reach higher energies are left out: arcs 3 to 6 will not be installed, nor will the so-called bypass needed in the final 50 GeV design to guide the beam outside the particle detector, which will only be installed in a later staging step. Beam spreaders and re-combiner modules will not be present in the first-stage lattice.

On the other hand, a number of key elements will define the geometry of the ERL from phase-one and remain untouched for all energy steps. The linacs, the interaction region (IR) and the beam separation scheme will be designed to be valid for any operation energy. As described in detail in [3] the proton and electron beams are separated after the interaction point through their different beam rigidities. A combination of a weak dipole field embedded inside the detector and the combined function effect of the off-centred mini-beta quadrupoles of the electron lattice acts as an effective separation scheme. The actual value of the dipole strength and the offset

of the quadrupoles were optimised for the lowest synchrotron radiation and thus equal effective bending radii in the three magnets [5], and for the phase-one scenario described here, the electron bending radius of this separation scheme is of about 1500 m.

However, while the geometry of the ERL will remain basically untouched, the impact on beam dynamics deserves closer investigation. Special emphasis is put on:

- p -optics, orbit / beta-function
- beam-beam effect on the proton beam / ditto for the electrons
- electron emittance
- luminosity reach
- beam separation scheme and synchrotron radiation
- polarisation
- cost savings

The interaction region of the ep collisions is shown schematically in Fig. 2.

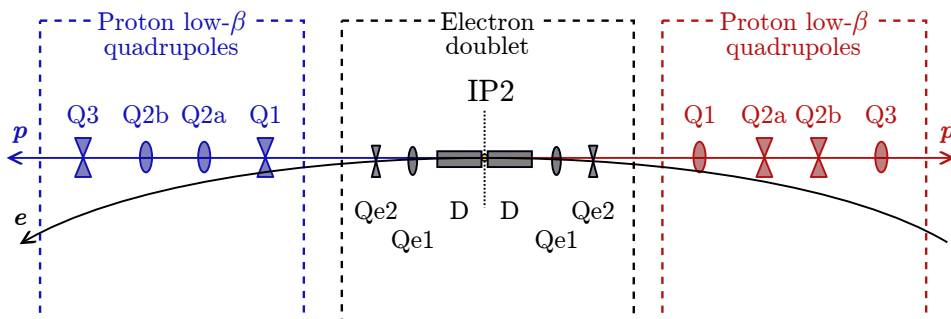


Figure 2. The interaction region of electron and proton beams: in black the mini-beta focusing scheme of the electrons is shown, including the detector dipole field that is part of the beam separation. Both are embedded within the free space of the HL-LHC proton inner triplet lattice, marked in blue and red.

p -optics, orbit / beta-function. While the electrons will be separated early enough and do not see any influence from the proton mini-beta quadrupoles, the proton beam on the other side will be distorted by the fields of the electron mini-beta quadrupoles. However, the influence on beam optics and orbit is weak and scales with the ratio of the energy of both counter-rotating beams. For the design case of the 50 GeV electron and 7 TeV proton beams, the effect has been calculated and the remaining distortions compensated; see Fig. 3. The so-called beta-beat, $\Delta\beta/\beta$ that reaches not more than 1.8% is locally corrected by a rematch of the neighbouring quadrupoles [3]. Reducing the energy of the electron beam to 20 GeV evidently also reduces this effect, and values of the order of 0.7% are expected at most. Compared to the overall budget of $\Delta\beta/\beta = 20\%$ for the LHC optics tolerance this is a negligible contribution; nevertheless, a correction is available and has been applied.

Beam-beam effect on the proton beam. The beam-beam interaction on the other side has a highly unbalanced effect, as it depends on the energy and the bunch

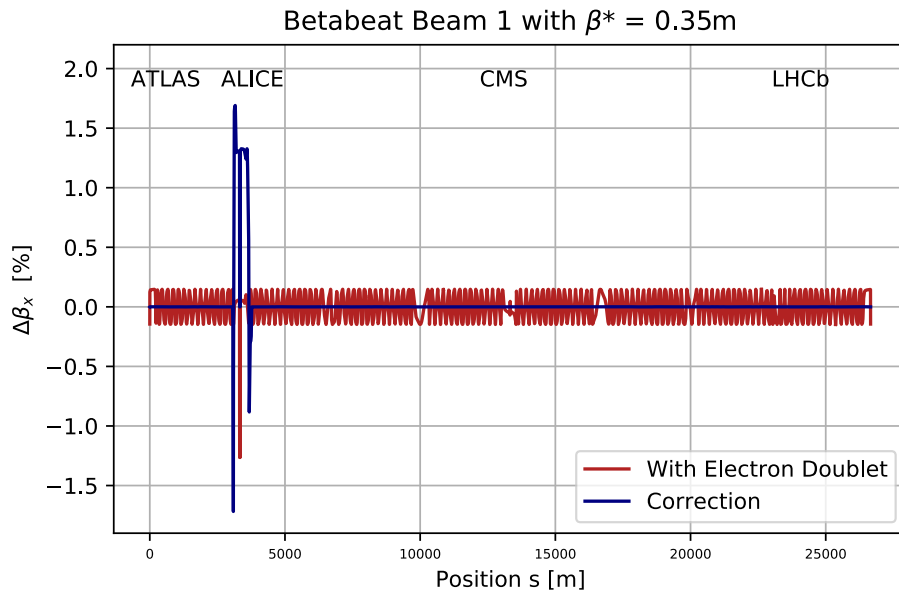


Figure 3. Local distortion of the proton optics due to the influence of the electron quadrupoles before (red) and after a local compensation of the effect (blue).

intensity of the opposing beam. In linear approximation the resulting tune-shift is given by:

$$\Delta Q_{x,y} = \frac{N_e r_0 \beta_{x,y}^*}{2\pi \gamma \sigma_{x,y} (\sigma_x + \sigma_y)}$$

where we refer here to the effect on the proton beam; accordingly N_e is the electron bunch population, r_0 the classical proton radius, γ is the electron Lorentz factor and β^* and σ are the amplitude function and beam size at the Interaction Point (IP). We would like to point out that in this approximation the tune-shift does not depend on the β -function. However, it depends on the energy of the beam considered. So in case of the protons, the resulting effect caused by the electron beam leads to a tune-shift of $\Delta Q_{x,y} \approx 3.8 \cdot 10^{-4}$, nearly two orders of magnitude smaller than the effect of the proton-proton interactions for the HL-LHC operation where we obtain $\Delta Q_{x,y} \approx -8.6 \cdot 10^{-3}$ per IP and thus the additional distortion due to ep collisions only has a marginal effect.

Beam-beam effect on the electron beam. However, the situation changes considerably for the electrons. Due to the lower beam energy the electrons are more sensitive, and especially the effect of the non-linear terms has to be minimised. In Fig. 4 the beam size of the electron beam is shown as a function of the position s along the beam orbit with $s = 0$ referring to the IP. In black, the theoretical beam size is plotted as it is obtained without beam-beam forces. The strong additional focusing due to the space-charge forces of the proton bunch is shown in blue. Here we would like to point out that the dominant parameter, the proton bunch population, refers to the ultimate goal of $N_p = 2.2 \cdot 10^{11}$ as foreseen for the HL-LHC luminosity upgrade. Under the influence of this additional focusing – called “pinch effect” – the electron beam

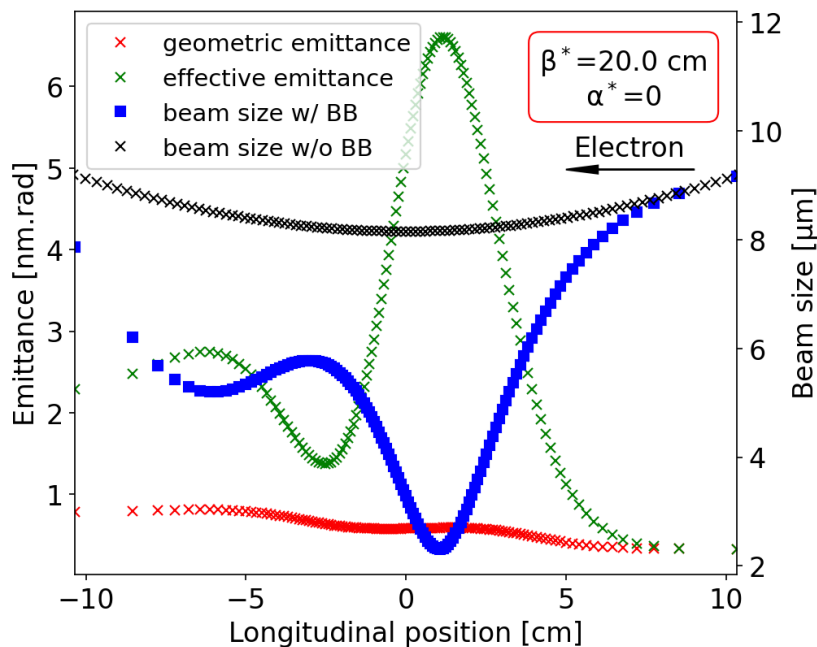


Figure 4. Effect of the space charge force on the 20 GeV electron beam: The beam size is reduced (leading to an additional enhancement of the luminosity, pinch effect) and re-matched to the ideal conditions before entering the return arc for energy recovery.

reaches a smaller effective beam size which is however to a large extent compensated by the so-called hourglass effect of the beam focusing in the vicinity of the IR. The optics distortion however has to be corrected in order to obtain well-matched beam parameters before entering the return arc and the decelerating process of the ERL. This is also highlighted in Fig. 4, where black and blue curves are indeed congruent before and after the interaction region. While this fact represents the prerequisite for a successful energy recovery, the non-linear terms of the beam-beam interaction are better visible in the phase-space representation. The situation for the two electron energies considered here, 50 GeV and 20 GeV, is compared in Fig. 5. As expected, the beam-beam effects for the lower-energy electrons are more prominent, and therefore stronger tails in the phase space distribution are developing during the beam-beam interaction. However, still due to the re-matched beam optics the large majority of the particles can be guided back through the decelerating part of the ERL and an energy recovery efficiency of close to 98% still is obtained.

Electron emittance. The above mentioned re-optimisation of the beam-beam interaction clearly involves matched beam sizes between electron and proton beam in both planes:

$$\sigma_{x,e} = \sigma_{x,p} = \sigma_{y,e} = \sigma_{y,p},$$

and thus the emittance of the electrons for the 20 GeV case has to be taken into account in a proper manner. In a storage ring the equilibrium emittance is well defined by the emission of synchrotron light. In the case of an ERL however, this equilibrium will never

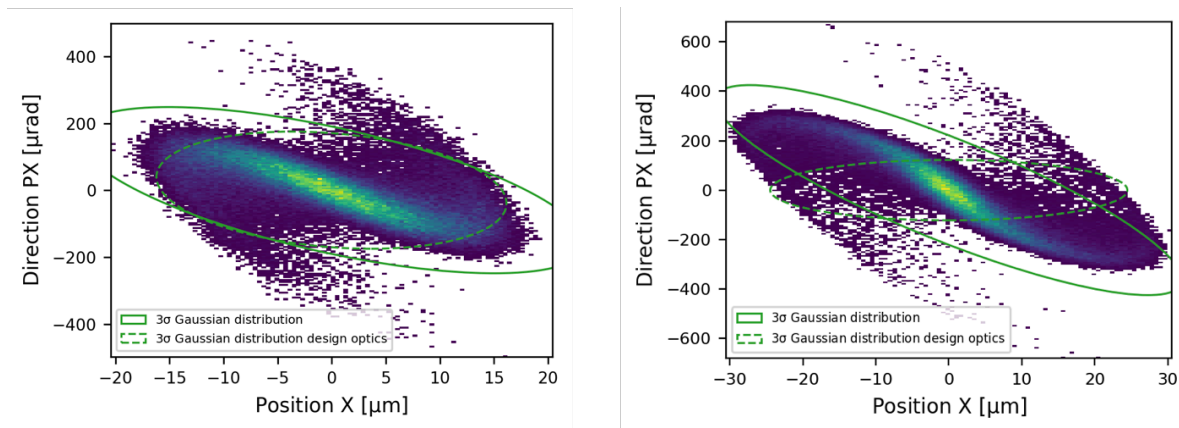


Figure 5. Visualisation of the beam-beam effect in phase space: in green the ellipse of the ideal configuration is shown. Due to the beam-beam effect, tails in the particle distribution are developing (blue spots) that have to be kept under control for full energy recovery performance. Left: 50 GeV case, right: 20 GeV. The lower energy of the 20 GeV electrons makes them more susceptible to the beam-beam force and the tails are more developed.

be reached. Ignoring the small effect of quantum emission in return arcs, the electron emittance therefore follows the rule of adiabatic damping $\varepsilon \propto 1/\gamma$. As a consequence, the emittance of the 20 GeV electron beam at the interaction point is considerably larger than the corresponding value at 50 GeV. This fact has to be taken into account to fulfil the matching condition for the transverse sizes between protons and electrons at the IP. In principle a strong reduction of the β -function would be needed to compensate for the increased beam emittance. However, this is far beyond the capabilities of the mini-beta quadrupoles.

In addition, the conditions of matched beam sizes for the 20 GeV phase-one scenario are obtained with electron beam optics that has been slightly adjusted for a β^* of 20 cm. Given the emittance and amplitude function of the colliding proton beam that define the optics conditions at the IP, we get a beam size at the ep interaction point of:

$$\sigma_p = \sqrt{\varepsilon_p \beta_p^*} = \sqrt{(3.3 \cdot 10^{-10} \text{ m} \cdot \text{rad}) (35 \text{ cm})} = 10.7 \text{ } \mu\text{m}$$

and the electron beam has to follow this condition.

For the amplitude function of the electrons, $\beta^* = 20 \text{ cm}$ we obtain a required absolute (i.e. geometric) electron emittance of $\varepsilon_0 = 5.7 \cdot 10^{-4} \text{ mm} \cdot \text{mrad}$. This corresponds to a normalised (energy independent) value of $\varepsilon_n = 22 \text{ mm} \cdot \text{mrad}$ and lies well within the specifications of the proposed particle source for the ERL [1]. According to the design parameters of the electron gun a normalised emittance even as low as $\varepsilon_n = 6 \text{ mm} \cdot \text{mrad}$ is expected (see Tab. 1) which represents a comfortable safety margin for the 20 GeV design.

In these considerations, the small effect of the emittance increase in the return arcs of the ERL was taken into account. Given the lower beam energy of 20 GeV, the emitted quanta have a much smaller effect, and the resulting emittance dilution remains at a

Table 1. General specification of the LHeC ERL electron source.

Parameter	Unit	Value
Booster energy	MeV	7
Bunch repetition rate	MHz	40
Average beam current	mA	60
Bunch charge	nC	1.5
RMS bunch length	mm	3
Normalised transverse emittance	mm·mrad	< 6
Uncorrelated energy spread	keV	10
Beam polarisation		Un-polarised/polarised

very low level of a few percent.

Beam separation scheme and synchrotron radiation. The beam separation between electrons and protons is provided by the combined effect of the detector weak dipole field and the off-centred quadrupoles of the electron mini-beta concept. Marked in blue in Fig. 2 the combined function quadrupoles of the doublet and the dipole field of the detector represent a bending force with equal and constant bending radius. They provide a smooth separation effect because of the different beam rigidities of electron and proton beams with a minimised critical energy and limited power of the emitted synchrotron light. Applying this scheme to the case of 20 GeV electron energy, results in small values of the emitted light and thus leads to a comfortable situation with $E_{\text{crit}} \approx 10$ keV and an overall radiated power in the interaction region of well below 1 kW.

Yet, another slightly modified beam separation scheme is possible: the strong dependence of synchrotron radiation on γ allows for the 20 GeV case a much stronger bending as the power of the emitted radiation scales as $P_\gamma \propto \gamma^4/\rho^2$ where ρ is the bending radius of the electrons. As a consequence, the applied bending fields can be increased considerably, allowing the electron beam to be guided outside the cryostat of the first proton quadrupole, labelled as Q1 in Fig. 2.

We would like to point out, however, that in any case a certain contribution of the dipole field to the separation is needed to avoid parasitic encounters of the counter-rotating bunches. Following the bunch spacing of the LHC, $\Delta t = 25$ ns, parasitic collisions will occur every 3.75 m and in order to avoid those the beams either have to be brought into collision under a crossing angle (which involves crab cavities to compensate the geometric luminosity loss) or – as foreseen in this scenario – a separation dipole field has to be applied right before and after the collision point, with the total bending power of at least 0.3 Tm.

Cost savings. Following the idea of a design that can be easily extended in energy by staging additional return arcs, the basic layout of the ERL will remain the same. However, starting with one-turn ERL the return arcs 3 to 6 as well as the so-called beam

spreaders and re-combiners at the end of the linacs and the bypass that guides the low-energy beam outside the particle detector will not be needed. A cost estimate for the original ERL design results in the budget of magnet and vacuum system of 11 kCHF per metre [6]. As a result, an overall budget reduction of at least 70 MCHF is obtained for the 20 GeV version discussed here. In addition, the lower electron energy allows a much simplified design of the interaction region – in the baseline case, with $\rho \approx 1500$ m, the synchrotron radiation is relatively weak and does not require installation of sophisticated protection masks and absorbers. In the alternative design with a faster beam separation, using $\rho \approx 120$ m, the corresponding orbit of the electrons can be guided outside the cryostat of the first superconducting proton quadrupole, located at a 23 m distance from the interaction point, and as a result, the layout of the IR in this case is fully compatible with the existing LHC mini-beta scheme, and a new magnet design for the protons (eventually based on Nb₃Sn technology) is not required for this phase-one scenario. The estimated additional cost savings are about 100 MCHF. Last but not least, the operating costs of the 20 GeV ERL will be much smaller with respect to the 50 GeV case because of much lower energy losses due to synchrotron radiation and the absence of the arc 3–6 beamlines.

As discussed in the 2021 CDR revision of the LHeC study [1] the installation of the ERL machine can be made partially in parallel during the Run4 operation period and the detector installation would then take place during the fourth Long Shutdown (LS4) planned in 2035-2036. In total, 7 years are needed to build the LHeC, including permits, engineering studies, tendering and land negotiations, and the final year of connection to HL-LHC [7]. Therefore, given a much simpler design of the phase-one LHeC proposed here and a timely decision on the start of such a project, we believe that the electron-hadron collisions can be available during Run5 of the HL-LHC.

Luminosity reach. The operational scenario for phase-one of the LHeC foresees a truly concurrent running of the ep operation in parallel to the standard HL-LHC proton collisions. As a consequence, the performance of the LHeC depends directly on the HL-LHC design parameters, mainly the frequency of bunch collisions f_{coll} , bunch populations N_e and N_p , and the achievable beta function at the IP. In the case of round beams and matched beam sizes, luminosity \mathcal{L} is given by:

$$\mathcal{L} = \frac{N_e N_p f_{\text{coll}}}{4\pi \varepsilon_p \beta_p^*} \Pi_i(H_i),$$

where the correction factors for hourglass and pinch effects and for the bunch filling fraction compensate each other, so in a good approximation one expects $\Pi_i(H_i) \approx 1$. It shows that luminosity is basically defined by the achievable amplitude function of the proton beam at the interaction point β_p^* . Thus, for a given beam size of the protons at the IP, we assume that the optics of the electrons in the ERL beam delivery system will follow, and the limiting factors are the available free aperture of the proton mini-beta quadrupoles and the dynamic effects created by the sextupole fields needed for chromaticity correction.

The values shown in Tab. 2 summarise the situation, with the nominal proton bunch

population, $N_p = 2.2 \cdot 10^{11}$ and the electron beam current in the ERL, $I_e = 60$ mA, which corresponds to $N_e \approx 10^{10}$ electrons per bunch.

It should be emphasised that the case described here refers to the truly concurrent operation of electron-hadron and hadron-hadron collisions. So, the aperture needed in the mini-beta quadrupoles of the protons is defined by both the colliding and the non-colliding proton beam. Therefore the “other”, non-colliding proton beam still has to be kept in the storage ring and guided through the ep interaction region untouched. However, in order to save free aperture for the optics of the colliding protons, relaxed beam optics has been developed which allows for minimum beam size and aperture need in the mini-beta quadrupoles: $\beta^* = 24$ m has been found as optimum value for the non-colliding proton in this case.

The same collision scheme will be applied for the other electron-hadron collisions. For example, assuming the nominal lead beam parameters at the HL-LHC, i.e. the beam radius of $17 \mu\text{m}$ and the Pb bunch population of $1.8 \cdot 10^8$, one expects the ePb luminosity at the LHeC of $2 \cdot 10^{30} \text{ cm}^{-2}\text{s}^{-1}$, or about $4 \cdot 10^{32} \text{ cm}^{-2}\text{s}^{-1}$ per nucleon.

Polarised electron beams can rather naturally be incorporated in an ERL type accelerator. Laser driven state of the art electron guns provide polarised beams up to 90% as previously suggested in the LHeC CDR [1]). Harmful effects like resonant depolarisation that play a major role in storage rings are by definition not existent and the de-tuning of the spin precession due to the emitted synchrotron light is estimated to be on the order of a few percent. As a consequence the acceleration chain provided by the ERL is quasi spin transparent and does not play a large role in the final – longitudinal – electron beam polarisation at the IP.

3. Physics case

In phase-one LHeC, the centre-of-mass energy for electron-proton collisions $\sqrt{s_{ep}} = \sqrt{4E_e E_p} = 0.75$ TeV, in place of 1.2 TeV for the 50 GeV electron beam at the final LHeC. This means that the kinematic reach on the $x - Q^2$ plane will already be greatly extended with respect to the data taken at HERA at $\sqrt{s} = 0.3$ TeV, as $Q_{\text{max}}^2 \simeq s_{ep}$ and $x_{\text{min}} \propto 1/s_{ep}$. As discussed in the LHeC CDR [1], a relatively low integrated luminosity of 50 fb^{-1} is sufficient to greatly improve the constraints on the parton density functions, particularly at low x . Therefore, already after two years of running the phase-one LHeC it will be possible to provide valuable feedback to hadron-hadron

Table 2. Luminosity reach in ep collisions for an electron beam energy of 20 GeV and the optimal proton optics definition, assuming a 60 mA electron beam current.

	p	e^-
Colliding beam β^* [cm]	35	20
Emittance ε [10^{-10} m · rad]	3.3	5.7
IP beam size σ^* [μm]	10.7	
Luminosity [$10^{33} \text{ cm}^{-2}\text{s}^{-1}$]	6	
Magnet technology	NbTi	

experiments at the HL-LHC, what will result in significant improvements in a number of precision measurements [7]. Moreover, with entering into a new kinematic region of very low x the novel QCD phenomena are expected to be observed – new parton dynamics and non-linear parton density effects.

Table 3. Inclusive Higgs, single top, and top pair generator level production cross sections for the phase-one and final LHeC, and for un-polarised and polarised electron beams. All cross sections are quoted at leading order, with the Higgs boson mass of 125 GeV and the top quark mass of 172 GeV.

Proton energy, E_p	7 TeV			
	50 GeV		20 GeV	
Electron energy, E_e				
Electron polarisation, P_e	0	−0.8	0	−0.8
$\sigma(e^-p \rightarrow H\nu_l + \text{jet} + X)$ [fb]	73	164	21	52
$\sigma(e^-p \rightarrow e^-H + \text{jet} + X)$ [fb]	14	19	3.4	5.6
$\sigma(e^-p \rightarrow e^-t\bar{t} + X)$ [fb]	26	28	0.93	0.99
$\sigma(e^-p \rightarrow \nu_l\bar{t} + X)$ [pb]	1.7	3.1	0.28	0.51

To illustrate the scientific potential of the research in electroweak and Higgs physics at the phase-one LHeC, a few MadGraph5_aMC@NLO [8] generator-level cross sections for un-polarised and longitudinally polarised electron beams are compared in Tab. 3 to those for the final LHeC. The Higgs boson case remains compelling at 0.75 TeV (especially for the charged current events), as well as the single-top-quark one, not only for mastering pioneering electron-proton measurement techniques but also for making measurements of some specific channels. For example, assuming the Run5 total integrated luminosity of 250 fb^{-1} at 0.75 TeV, and an 80% electron longitudinal polarisation, one obtains the following uncertainties by scaling up the errors obtained for the 1.2 TeV LHeC [1] using the numbers of produced events: $\delta\kappa_W \approx 2.5\%$, for the Higgs boson coupling to W bosons, and $\delta\mathcal{R}e(f_L^2) \approx 0.2$, for the anomalous Wtb coupling – both errors comparable to the expected final uncertainties for the corresponding measurements at the HL-LHC using 3 ab^{-1} of the proton-proton data.

In Fig. 6 we show the differential cross-sections in rapidity for the Higgs boson and a single top quark produced at the phase-one LHeC as well as the final one – for the latter the cross-sections peak at about $Y = 2$ requiring a good coverage in the forward part of the hadron hemisphere.

Experimental conditions at the LHeC will be particularly favourable for studies of the exclusive production via photon-photon fusion, the event pile-up will be negligible, highly improving the efficiency and purity of exclusive event selection, and at the same time some sources of overwhelming backgrounds, as due to the Drell-Yan process for example, will be absent. Moreover, no event suppression will occur due to hadronic re-scattering and the associated significant theoretical and experimental uncertainties

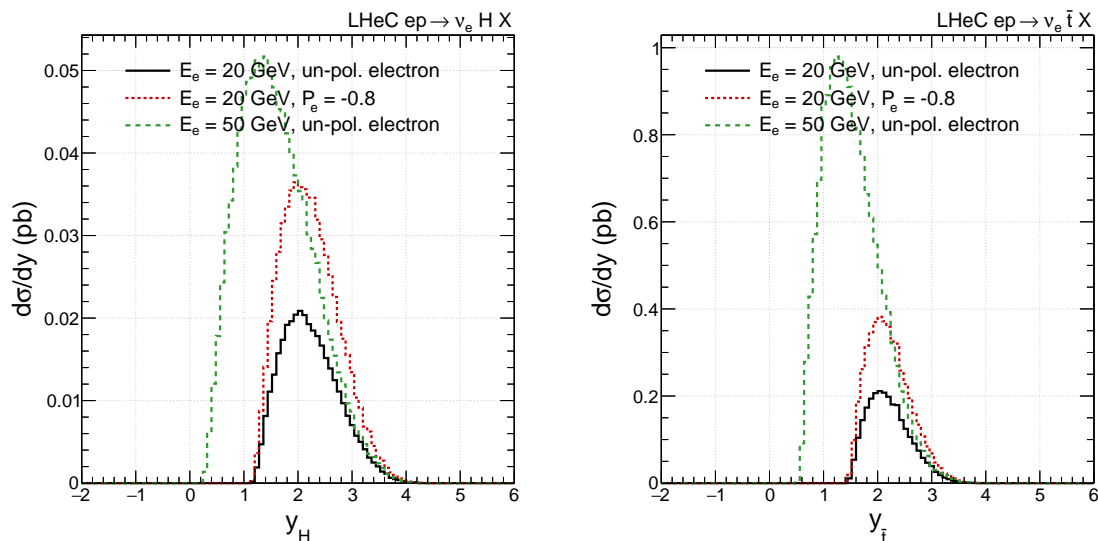


Figure 6. Differential cross-sections in rapidity for the Higgs boson (left) and a single top quark (right), both produced through charged current, assuming the phase-one electron energy of 20 GeV, with and without electron polarisation, as well as for the final energy of 50 GeV.

will not intervene. Finally, data streaming (or the absence of triggering) will allow for detection and reconstruction of a much wider range of final states. As a result, despite the lower average $\gamma\gamma$ centre-of-mass energy than that at the HL-LHC, a significantly larger statistics of detected photon-photon interactions is expected already at the phase-one LHeC.

The prime example is the two-photon production of W -boson pairs: assuming an integrated ep luminosity of 250 fb^{-1} , about 5000 pairs will be produced at 0.75 TeV [9]. As the semi-leptonic decays will be detected with high efficiency, that will lead to much improved sensitivities to anomalous couplings with respect to the measurements at the HL-LHC.

A fully exclusive two-photon production of tau-lepton pairs has a large cross section of about 40 pb at the phase-one LHeC, for pair invariant masses above 10 GeV [9]. This will lead to very large event statistics within the acceptance of the central detector and as a consequence to excellent sensitivity to the τ anomalous magnetic moment a_τ . With an integrated ep luminosity of 250 fb^{-1} , the expected sensitivity is an order of magnitude better than that achieved at the phase-one LHC. As a result, for the first time the experimental uncertainties will be better than the higher-order corrections to the τ magnetic moment in the Standard Model. Similarly, large improvements will be achieved in constraining the electric dipole moment of tau-leptons.

Last but not least, already at the phase-one LHeC, also one of the key questions in nuclear physics can be addressed: how the nucleon structure is modified when immersed in a nuclear medium. For example, by a precise measurement and complete unfolding of the distributions of all parton species in a single nucleus comparable to that in the

proton, the LHeC will revolutionise our understanding of nuclear structure in crucial and unique kinematic regions [1, 7]. In addition, it will allow to clarify the dynamics for particle production in nuclear collisions in the region of relevance for the LHC. Finally, it should be stressed that the phase-one LHeC provides an important opportunity to perform eA and AA measurements using the same detector.

4. General detector requirements

In 2022, an extension of the ALICE experiment beyond Run4 at the HL-LHC was proposed in a letter of intent [10]. In that document, two configurations of magnetic field were considered for the new ALICE 3 detector at the IP2 – produced either by the cost effective 7.5 m long solenoid, or by the high-performance combination of a 2.5 m solenoid at the centre with two 2 m long dipoles on its each side. As discussed above, to allow for electron-hadron collisions, the dipole field is necessary for the separation of the electron beam, so the latter approach is desirable in this context.

The most recent ALICE 3 design includes a good-performance tracking detector that covers a wide rapidity range of $|\eta| < 4$ [11], which is well compatible with the needs for electron-hadron measurements at the stage-one LHeC. However, in contrast, the present design lacks a hadronic calorimeter (HCAL) while a performant one is obligatory for achieving proper measurements of the DIS charged current events and reconstruction of the decays of top quark, Higgs, W and Z bosons. Moreover, an extension of the electromagnetic calorimeter is desirable in the electron forward direction to ensure a good reconstruction of DIS neutral current events, and in addition, important studies of exclusive production at the LHeC will largely benefit from specialised near-beam detectors in very forward electron and proton directions.

Finally, it should be stressed that the ALICE 3 design already contains a full data streaming mechanism (i.e. a "trigger-less" data acquisition), which is also very profitable for measurements at the LHeC.

In summary, it seems that the proposed ALICE 3 detector requires relatively small modifications, apart from the addition of HCAL, to make it also appropriate for the phase-one LHeC experiment – in this way, allowing to vastly increase the scientific scope and impact of research performed using the Run5 data.

5. Conclusions

In this paper, we argue that the phased implementation of LHeC is feasible and offers the best approach. Firstly, in this case the project financial load will be distributed over more years. Secondly, the experience acquired during the first stage of the project will allow a better design of the final LHeC and possibly also allow for its earlier startup. Finally, phase-one LHeC will ensure very important and timely scientific feedback to the hadron-hadron experiments at the HL-LHC, already during Run5.

The conceptual studies presented above demonstrated the high luminosity

performance of such a phase-one LHeC. This in turn guarantees excellent scientific output, including very interesting comparative studies of the eA and AA interactions, as the proposed IR design allows for both types of collisions at IP2.

The new detector at the P2 site can be designed by extension of the ALICE 3 proposal, which offers strong synergies and benefits in several aspects – for example, it is expected to result in its better performance and richer scientific output for studies of AA interactions.

Acknowledgements

L. Forthomme and K. Piotrkowski appreciate the financial support of the Polish National Agency for Academic Exchange (NAWA) under grant number BPN/PPO/2021/1/00011. L. Forthomme has also been supported by the NCN grants 2022/01/1/ST2/00022 and 2023/49/B/ST2/03273, and by the AGH IDUB and the CERN COAS programmes.

Bibliography

- [1] Agostini P *et al.* (LHeC, FCC-he Study Group) 2021 *J. Phys. G* **48** 110501 (*Preprint* 2007.14491)
- [2] André K D J *et al.* 2022 *Eur. Phys. J. C* **82** 40 (*Preprint* 2201.02436)
- [3] Holzer B J, André K D J, Armesto N, Bogacz S A, Hanstock D, Hounsell B, Klein M, Kostka P, Smith M W R and von Witzleben T 2022 *PoS ICHEP2022* 057
- [4] Bogacz S A, Holzer B J and Osborne J A 2023 *PoS* 305–320 (*Preprint* 2206.07678)
- [5] Andre K D J 2022 *Lattice Design and Beam Optics for the Energy Recovery Linac of the Large Hadron-Electron Collider* Ph.D. thesis Liverpool U.
- [6] Bruning O 2018 LHeC cost estimate Tech. rep. CERN Geneva URL <https://cds.cern.ch/record/2652349>
- [7] Ahmadova F *et al.* 2025 (*Preprint* 2503.17727)
- [8] Alwall J, Frederix R, Frixione S, Hirschi V, Maltoni F, Mattelaer O, Shao H S, Stelzer T, Torrielli P and Zaro M 2014 *JHEP* **07** 079 (*Preprint* 1405.0301)
- [9] Forthomme L, Khanpour H, Piotrkowski K and Yamazaki Y 2025 *In preparation*
- [10] Acharya S *et al.* (ALICE) 2022 Letter of intent for ALICE 3: A next-generation heavy-ion experiment at the LHC Tech. rep. CERN Geneva (*Preprint* 2211.02491) URL <https://cds.cern.ch/record/2803563>
- [11] Dainese A and Di Mauro A 2025 Scoping document for the ALICE 3 detector Tech. rep. CERN Geneva URL <https://cds.cern.ch/record/2925455>